IOP Publishing
Measurement Science and Technology
Meas. Sci. Technol. **31** (2020) 045405 (7pp)
https://doi.org/10.1088/1361-6501/ab5002

Digitally controlled deflection of an electron beam with a miniature octupole unit

Marcin Białas, Artur Wiatrowski and Witold Słówko

Faculty of Microsystem Electronics and Photonics, Wroclaw University of Science and Technology, Janiszewskiego 11/17, 50-372 Wroclaw, Poland

E-mail: marcin.bialas@pwr.edu.pl

Received 25 June 2019, revised 16 October 2019
Accepted for publication 22 October 2019
Published 17 January 2020

Abstract

The paper describes results of preliminary investigations of an octupole deflecting-focusing system, comprising a miniature unit of two diaphragms: a focusing diaphragm divided into eight segments with an octupole axial symmetry and a screening diaphragm. They are electrically isolated and can be mutually biased up to ±4 kV with focusing voltage, while an isolated sample stands for the third electrode of a unipotential focusing lens. The octupole unit is steered by a digital, eight-channel electronic control system with isolated output circuits, enabling high-voltage bias of the octupole focusing diaphragm. The system is destined for handling an ion beam from a coaxial ion micro-source in scanning electron microscopy or an electron beam in a prospect electron optical micro-device. Preliminary tests conducted with a JSM-840 scanning electron microscope proved that the quasi-planar deflecting and focusing system (2.5 mm thick, at a distance of 3 mm to the sample) is capable at operating with acceptable imaging errors. Further, the electronic control system and the software fully meet the requirements.

Keywords: octupole, micro deflection and focusing unit, steering circuits

(Some figures may appear in colour only in the online journal)

1. Introduction

Electron beam deflectors, or rather beams of charged particles, are the most important parts of electron (or ion) optical instruments. They should produce a highly homogenous dipole field perpendicular to the beam axis. Electrostatic or magnetic dipole fields can both be used: while magnetic deflectors offer stronger deflection force and lower aberrations in general, on the other hand electrostatic fields can give the same deflection angle both for electrons and ions independently on their atomic weight, so they are applied frequently in ion instruments such as focused ion beams (FIBs) [1, 2]. In addition, electrostatic deflectors usually present a relatively small size and can work in a much wider frequency band than the magnetic ones. In order to provide 2D scanning of a beam in the x and y directions, electrostatic deflectors consist of two pairs of plates with mutually orthogonal symmetry planes, positioned one after another along the beam axis. The large dimensions of the deflecting plates force designers of more compact structures to arrange the electrostatic deflector in the form of a tube much longer than its inner diameter and cut longwise in four segments. This shortens the deflector at least twofold but makes the inner electric field distribution undesirably inhomogeneous. Much better homogeneity can be achieved by cutting the deflector tube into eight equal segments (i.e. an octupole deflector) or even into 20 non-equal ones. The latter is easier to supply because it needs only one voltage supplier, while for octupole deflectors at least two are necessary.

The authors could not be satisfied with any of the above solutions because they had to design not only a miniature beam-deflecting unit but also a unit able to focus the beam dynamically and short enough to be placed in a gap between the objective and the sample stage of a scanning electron microscope (SEM) which should be shorter than 8 mm to provide good resolution. Such an arrangement would be desired by the authors for handling an ion beam produced by a coaxial ion micro-source designated for SEM [3]. A similar unit manufactured in micro-electromechanical systems technology is planned for a 'portable' scanning transmission electron microscope (STEM) [4].

The best solution would be a 2D octupole unit with its length reduced almost to 0, i.e. a quasi-planar one. What is more, the deflector structure should be entirely contained inside a unipotential lens, necessary to focus the charged particles beam on a sample and to play the role of a focusing diaphragm. This means that the deflecting function of the unit cannot be realised by a homogenous electric field in the space inside the plates because it does not exist. Instead, the beam deflecting must be conducted outside the plates in strongly inhomogeneous fields, frequently called 'fringing fields' [5]. Commonly, these parts of the deflecting field are reckoned sources of additional aberrations and in some designs are screened especially [6]. An encouraging example of a design applying fringing fields might be an electron gun monochromator developed by Mook and Kruit [7]. However, it also uses relatively thick main dipole fields at the very beginning of the electron optical system, which can reduce possible aberration discs. Thus our experiments were focused on two aims. Firstly, the complex beam controlling system should be checked, before the next steps of the project's realisation are undertaken. Secondly, experiments should test whether the beam deflecting in the 'fringing fields' causes acceptable image confusions. If not, the functions of the beam focusing and corrections of the field curvature and astigmatism will still remain to be addressed for the unit [8–10] and its steering system.

The features of a quasi-planar deflecting-focusing system could be tested in the arrangement of its destination, i.e. in combination with a coaxial ion micro-source arranged in SEM. In that case, ion beam diameters are usually measured with variants of the 'knife edge method' [11] developed previously for electron beams, or more sophisticated methods dedicated for FIB [12, 13]. However, the coaxial source can produce ion beams of tens of micrometers in diameter that result in resolutions too low to be used for imaging or defining aberrations of the system, which was important for its other possible applications as in for electron beams. Apart from deflecting, a main function of the system is beam focusing, so its electron optical features as a function of the focusing voltage should be measured. To obtain such possibilities, the authors applied SEM as a kind of an electron optical bench in which a pivotal point of the scanned beam was reckoned an imaged object but the place where its point-image arises could be calculated from the frame dimensions (i.e. a sample image magnification). For the measurements, the deflecting-focusing system was placed in a normal position to the ion source (it was out of operation), which corresponded better to its final function.

2. Octupole deflector design

The authors designed the octupole deflector in a form which enabled its accommodation in the sample chamber of the JSM-840 microscope used in experiments. In figure 1 a diagrammatic cross-section of the octupole unit and a view from its bottom are shown. The base of the deflector structure is a mounting disk (14 mm in diameter and 2 mm thick) made of FR4 laminate covered with Cu on both sides. The disk has a hole of 3 mm in diameter bored 2 mm aside of the disk axis, around which eight connecting paths have been etched symmetrically in the Cu layer on the bottom side and a conducting ring on the upper side. To obtain the octupole diaphragm, a disk of 5 mm in diameter made of 70 μm thick bronze foil was soldered to the eight connecting paths at the hole axis. Next, in the bronze disk a circular diaphragm (1.5 mm in diameter) was cut together with eight slots dividing the foil disk into eight mutually isolated segments of the octupole. The gaps between segments were so small (0.1 mm wide) that they could not disturb the axial symmetry of the focusing field. The latter operation was performed with the use of a laser plotter to obtain the necessary accuracy. Next, the screening diaphragm with an opening of 0.5 mm in diameter was soldered on an upper side of the mounting disk. Finally, wire leads in Teflon insulation were soldered to the connecting paths and secured from electric discharge with a mica disk (muscovite, 0.1 mm thick).

Thus, the octupole set consists of three parallel electrode units, i.e. the screening diaphragm and the octupole diaphragm unit electrically isolated with the mounting disk, which can be biased up to ±4 kV with a so-called focusing voltage, U_F; the third electrode is constituted by the sample holder, which is even better isolated from the microscope body to withstand a high voltage bias of a few kV. The three mentioned electrodes constitute an electron lens which may be arranged as a unipotential lens in the simplest case presented in the paper. Such a unit is expected to serve not only for the e-beam deflection but also for beam focusing and correction of astigmatism and field curvature errors. All these functions should be realised simultaneously thanks to dynamic biasing of the electrodes with the use of a digital control system.

3. Electronic control unit

The electronic control system may be reckoned a digital, eight-channel, high-voltage power supply [14], the settings of which can be changed over 1000 times per second. It consists of three main modules, shown in figure 1, i.e. an isolated analogue eight-channel block, a digital control block and a steering computer (PC1). The system also comprises a set of inner and outer supplies. A block diagram of the system is shown in figure 2. The common ground of the analogue block has been separated from the main ground of the system, which enables biasing it with a high voltage (the focusing voltage, U_F) up to ±4 kV, which adds to a constant component of all output voltages. Independent control of the potentials of the octupole electrodes in a range of ± 120 V allows deflection of the beam and errors correction, while the common bias, U_F, ensures focusing. The main constituents of the analogue block are eight WWN-02 output circuits (figure 3) which consist of two stages: an integrated differential amplifier and a main amplifier made of discrete components. The system gain is approximately 50 V V^{-1}, at a bandwidth of 8 kHz and the output current limited electronically to around 80 mA. Its amplitude (solid line) and phase (dashed line) diagrams are shown in figure 4. These result from simulations in the

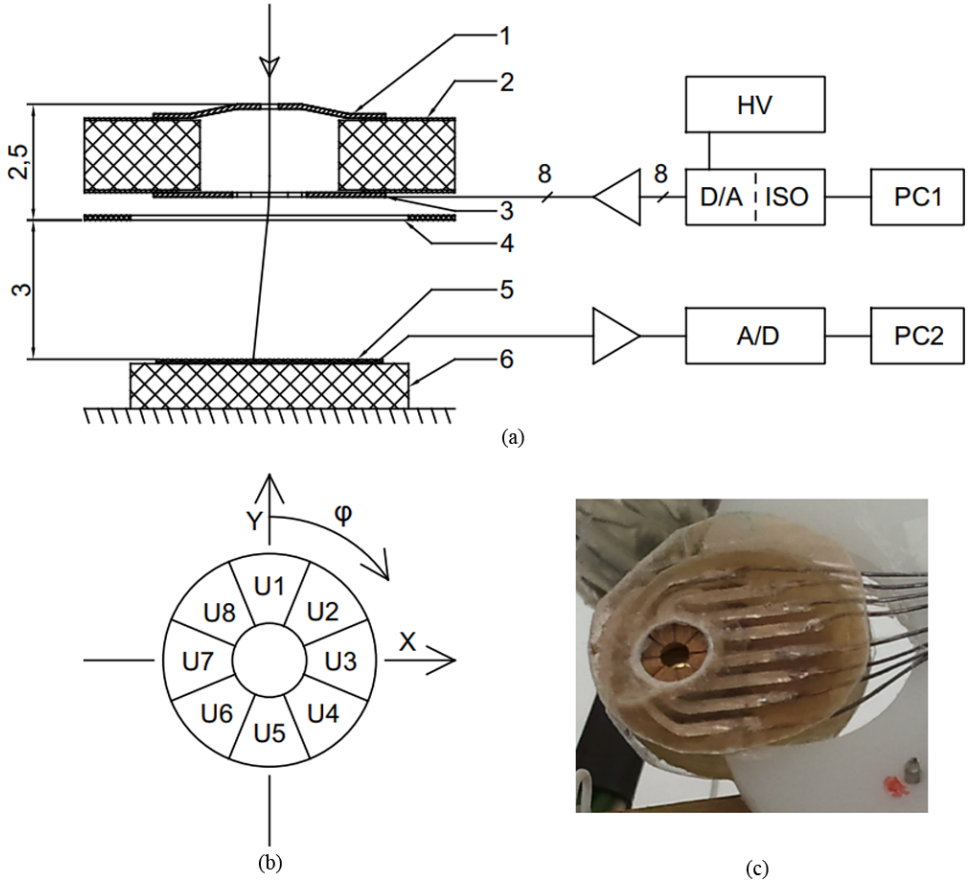

Figure 1. Octupole system: (a) scheme of the octupole system (1—screening diaphragm, 2—mounting disk, 3—octupole diaphragm unit, 4—mica disk, 5—sample holder, 6—sample isolator, D/A + ISO—isolated, digital analogue eight-channel block, PC1—steering computer, HV—high voltage supply for focusing voltage U_F, A/D—absorbed current meter and frame-grabber, PC2—imaging computer), (b) layout of the octupole electrodes (upside view), (c) assembled octupole unit.

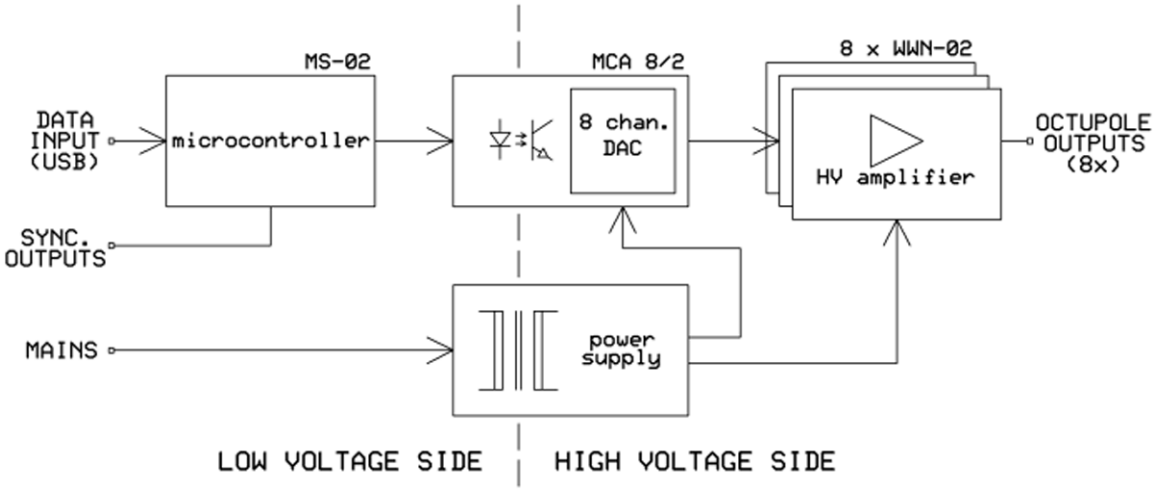

Figure 2. Block diagram of the electronic control system.

LTSpice IV program, but the same diagrams were measured in the real circuits.

A galvanic isolation of the analogue output block is ensured by a safety transformer in the supply module and a set of high-voltage optocouplers at the output of the digital control block (in the MCA8/2 module).

Digital signals obtained from the control block are sent to four two-channel digital to analogue (D/A) converters along with an addressing system and reference voltage sources and as analogue signals to the WWN-02 output circuits (with a 12-bit resolution). A block diagram of the DAC card is shown in figure 5. Potentiometers P1 and P2 in the reference voltage generator allow one to scale and shift the output voltage regulation range.

The digital control block constituted by a MS-02 steering unit with an Arduino UNO board is responsible for

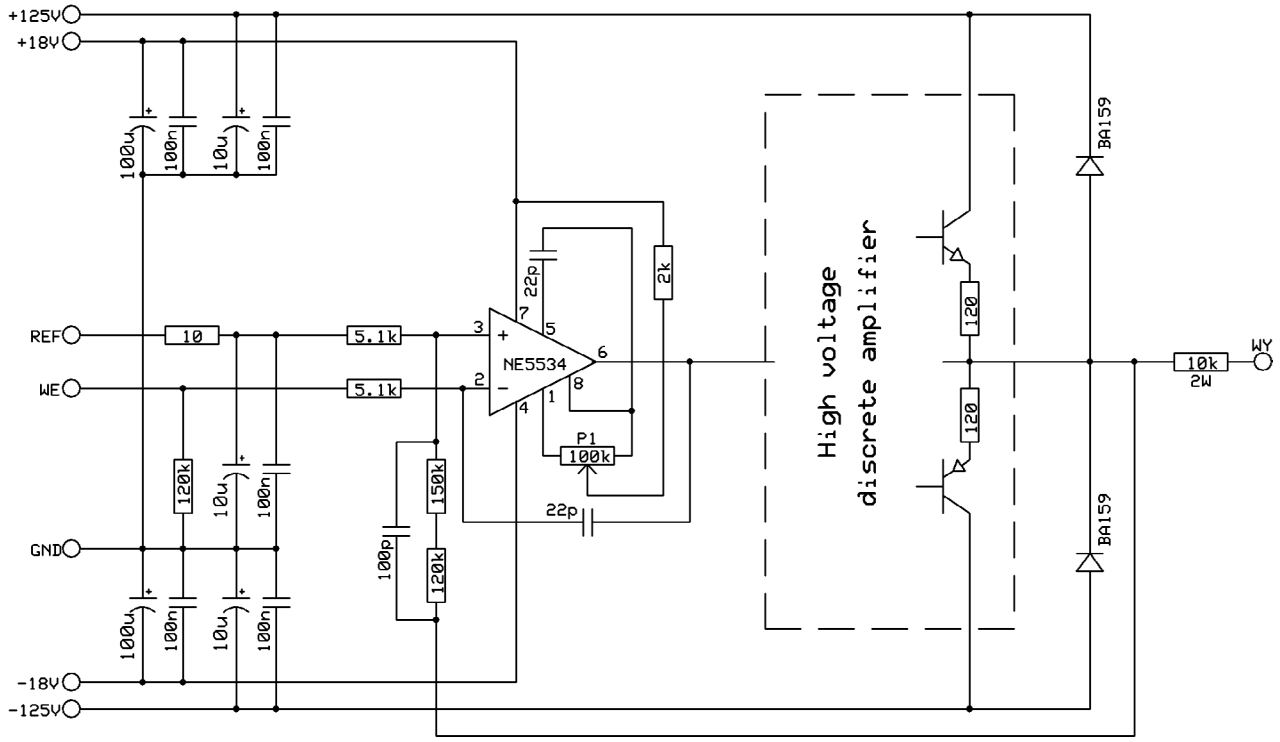

Figure 3. Simplified schematic of WWN-02 output circuits.

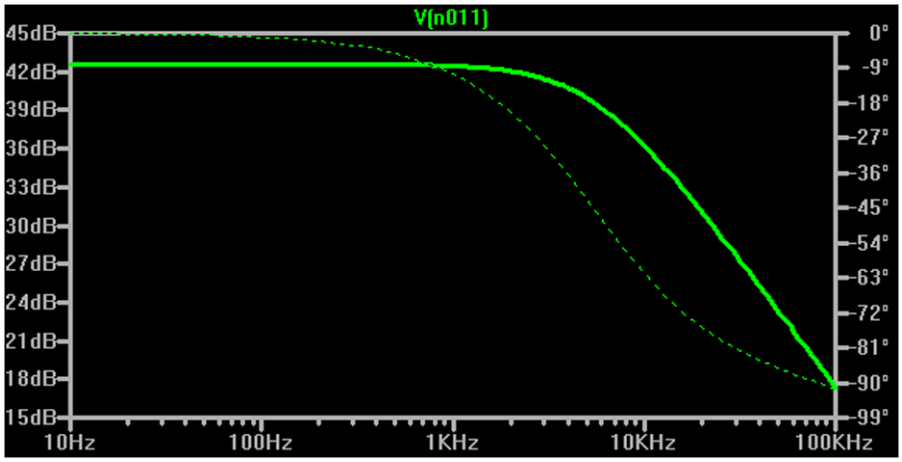

Figure 4. Signal amplitude (solid line) and phase (dashed line) versus frequency for the analog output module.

communication with the computer and internal circuits. It generates synchronization signals that can be used with measurement unit, and it can also support additional sequential memory. The latter speeds up the scanning and allows for very time-stable signals to be generated, which is impossible when transmitting settings directly from a computer.

The software for the microcontroller in the Arduino module was written in assembler language, whereas the program calculating the settings and operating on PC1 was written in LibertyBASIC. The control program enables working both in the raster scan and the vector scan mode, though codes for error compensation have been not developed yet. The latter needs vast investigations to establish the nature of the errors and their dependence on the unit settings. The vector scan mode seems more advantageous for the experiments conducted presently as deformations of geometrical figures generated in particular parts of the image may be some measure of the deflection errors.

The entire working range of the 12-bit D/A converters should cover the maximum radius of the working area (in the control program) equal to 2047 machine units (steps). A machine unit (step) is equal to the least significant bit in the D/A register. As the maximum voltage amplitude of the analogue output is ± 120 V, the output voltage maximum step is $u_s = 0.0586$ V/st.

Equations of electrode potentials were derived from analogous equations for magnetic potentials of the magnetic octupole [5]. When all constants were reduced to a single parameter u_s [V/step] and the beam deflection expressed as a number of deflection steps n (lateral or angular), very simple

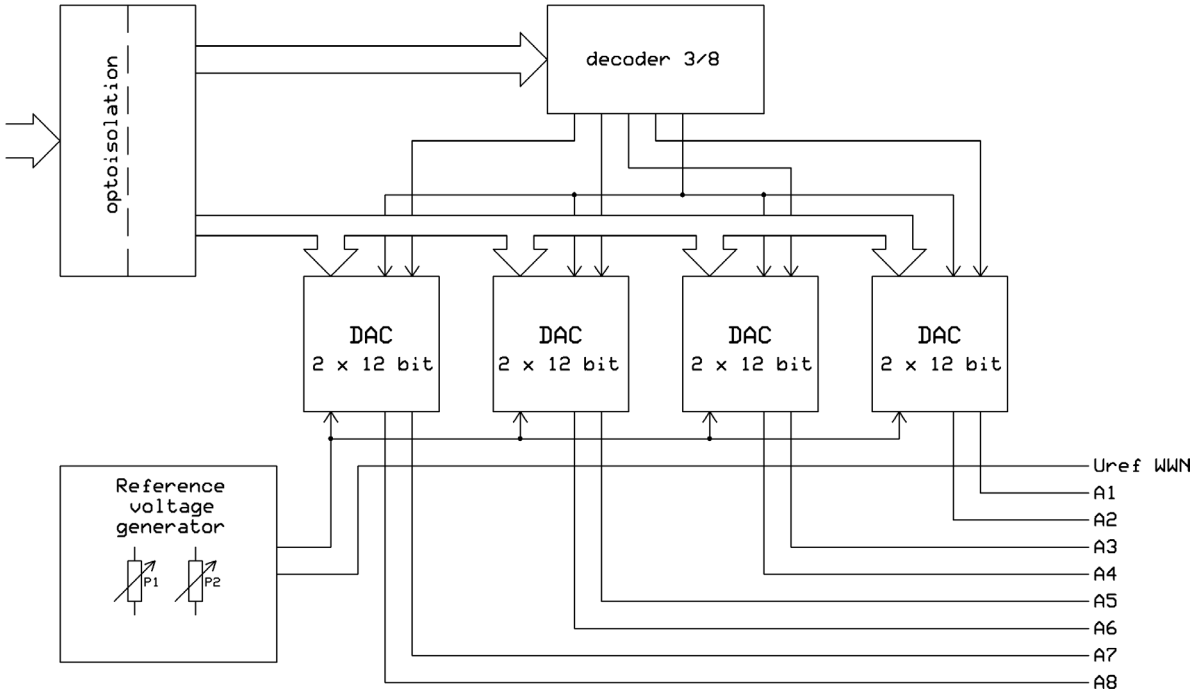

Figure 5. Block diagram of digital to analog converters (DAC) card.

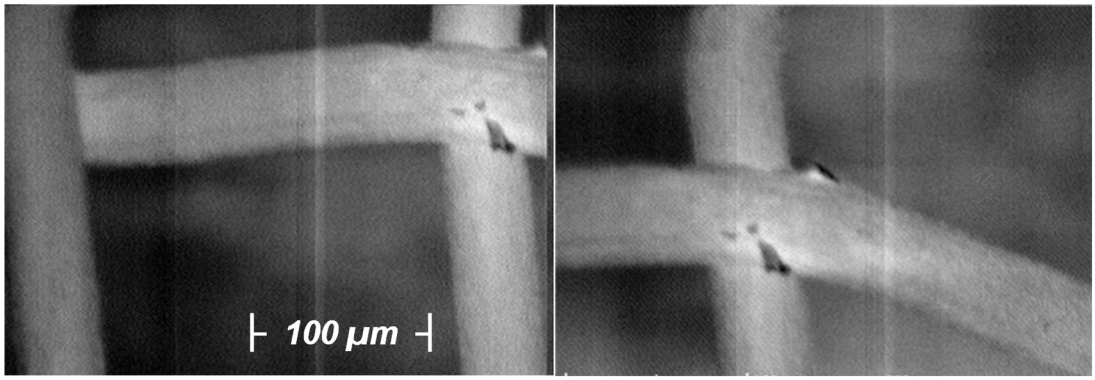

(a) (b)

Figure 6. Images of the molybdenum test grid acquired with the absorbed current channel (JSM840, $U_A = 4\,\mathrm{kV}$, $I_{EB} = 40\,\mathrm{nA}$; focusing voltage $U_F = 0\,\mathrm{V}$): (a) before deflection, (b) after deflection of 1500 steps (radial shift, $R = 0.15\,\mathrm{mm}$ on the sample plane, azimuth angle $\varphi = 245°$).

relationships for the electrode potentials were obtained in the polar coordinates:

$$U_1\,[V] = n\,[st]\,u_s\left[\frac{V}{st}\right]\cos\varphi, \tag{1}$$

and analogously:

$$U_3 = nu_s\sin\varphi \tag{2}$$

$$U_2 = \frac{U_1 + U_3}{\sqrt{2}} \tag{3}$$

$$U_4 = \frac{U_3 - U_1}{\sqrt{2}} \tag{4}$$

$$U_5 = -U_1 \tag{5}$$

$$U_6 = -U_2 \tag{6}$$

$$U_7 = -U_3 \tag{7}$$

$$U_8 = -U_4, \tag{8}$$

where φ is the azimuth angle of the deflected beam with respect to the y axis. The right values of the angular γ or lateral R deflections on the sample surface can be calculated as

$$\gamma = u_s n S_\gamma \text{ or } R = u_s n S_R, \tag{9}$$

and for rectangular coordinates

$$y = R\cos\varphi, x = R\sin\varphi, \tag{10}$$

where S_γ and S_R are the angular and lateral sensitivities of the deflection unit. Their values depend on the beam accelerating voltage and the distance to the sample as well as many other factors specific for the unit arrangement, so they should be established experimentally for each case.

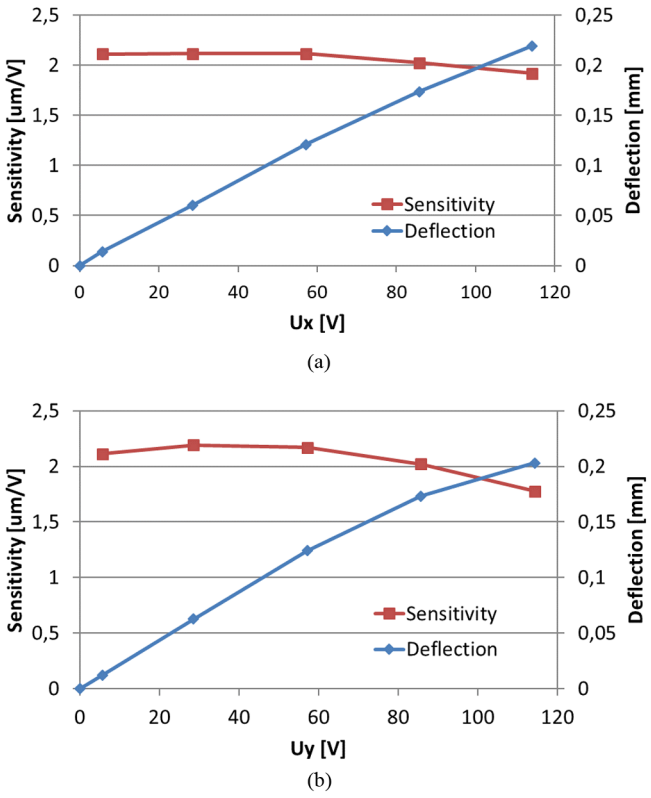

Figure 7. Image deflection and the deflection sensitivity in the x, y axes as a function of the axis deflection voltage (for $U_F = 0$ V): (a) in the x axis, (b) in the y axis.

4. Experiments

As is seen in figure 1, the octupole deflection unit is 2.5 mm thick and positioned at a distance of 3 mm from the sample surface, which makes the whole structure some 5.5 mm thick. The electrostatic deflection sensitivity observed in a standard cathode ray tube (CRT) is proportional to the deflection plate length and their distance to a screen. The sensitivity is reverse proportional to the beam energy, which was taken as 4 keV maximally for the limited voltage endurance of the mounting disk. The miniature length of the structure and relatively high energy of the beam must make the deflector sensitivity very low. In these circumstances, the authors decided to arrange the testing system based on a JSM-840 SEM.

The octupole unit is 14 mm in diameter and leaves only 3 mm distance between the sample and the octupole diaphragm. The latter may be biased with a focusing voltage up to −4 kV, which entirely blocks flow of secondary electrons (SE) and backscattered electrons (BSE) of lower energies to the standard signal detectors. Then, images of the sample were synthesized of the specimen-absorbed current acquired by an autonomous image acquisition system. The latter comprised a home-made preamplifier and analogue to digital (A/D) converting frame grabber connected to personal computer (PC2) displaying the image on its screen. The image displacement due to the beam deflection (as shown in figure 6) was compensated by the sample stage movement with micrometric screws (with an accuracy of 5 μm), which was the measure of the deflection. This way, a row of errors coming from the electron optical system could be eliminated. To obtain acceptable image quality the sample current had to be relatively high (30 nA ÷ 70 nA). This was a challenge for the tungsten cathode at the accelerating voltage, $U_A = 4$ kV, and required the SEM aperture to be removed. The authors were also unable to ground firmly the signal preamplifier to the high-voltage part of the control unit biased with a few kV, and images were confused by the 'buzz' from the control unit supply (visible in figure 6). After numerous trials, a rectangular grid made of molybdenum wires, 50 μm thick disposed with 250 μm pitch, was chosen as a test object for imaging. Despite all the obstacles, the images are clear enough to state that the quadrupole deflector does not cause noticeable image aberrations, at least in its basic state of work, i.e. with a focusing voltage $U_F = 0$ V.

Measurements of the deflection linearity and sensitivity in the main directions, shown in figure 7, are also rather optimistic. Differences between sensitivities measured for the minimum and maximum deflections in the x and y directions come to *ca*. 10% and 20% for each direction, respectively, but the mutual differences between them do not exceed 7.6%. A maximum sensitivity of 2.2 μm V^{-1} seems very low but should be compared with the minute thickness of the octupole (70 μm), which can easily be enlarged without serious changing of the whole structure length. The differences of the sensitivity and linearity in the x and y directions are probably caused by the disturbed symmetry of the whole structure, associated with its hand-making without special instruments.

Next, measurements were conducted to find the influence of the focusing voltage U_F on the beam deflection; their results are shown in figure 8. In this case, the octupole structure represents a unipotential lens with a retarding inner electrode because the octupole focusing diaphragm is biased negatively. According to the diagram, the beam deflection increases very slowly as the focusing voltage decreases to obtain an asymptote for $U_F = -3.2$ kV. In this range the deflection sensitivity should increase reverse-proportionally to the decreasing energy of electrons near the octupole diaphragm. This, however, is partly compensated by the increasing focusing power of the lens, which also affects the dimensions of the SEM raster and magnification of its image. At the asymptote voltage the lens imagines a pivot point of the scanned beam on the test grid plain so the scanning frame is reduced to a point and the image magnification goes to infinity, which makes it unresolvable. For still lowered U_F, images of the pivot point are created above the test plain and get reversed but have finite dimensions and resolvable details. The octupole lens also influences the electron beam focusing, and the SEM objective lens must be properly weakened to obtain a sharp image of the test grid.

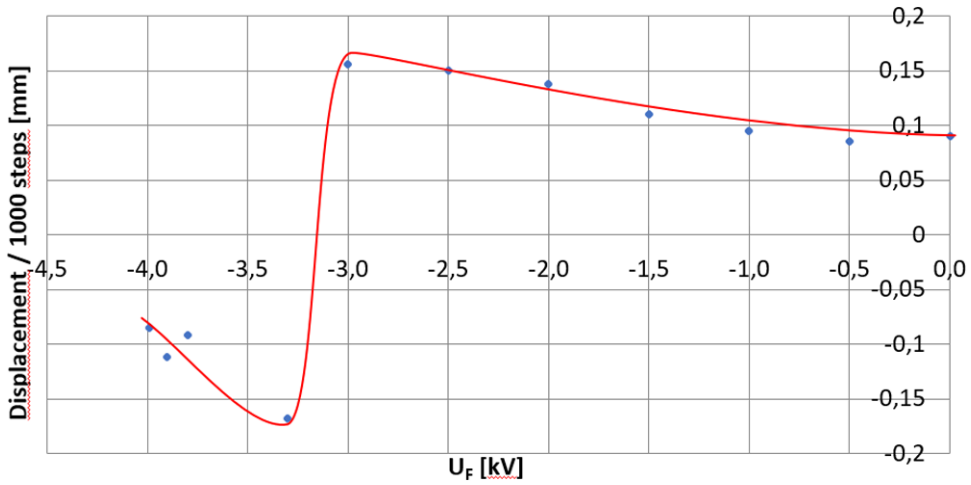

Figure 8. Image deflection in the x direction for 1000 steps as a function of the focusing voltage U_F.

5. Conclusions

The results of the preliminary experiments presented above seem rather optimistic. The main purpose of this undertaking was to prove that a quasi-planar deflecting and focusing system is capable of operating with acceptable imaging errors. Images displayed in figure 6 suggest a lack of noticeable image deformations after its deflection to three quarters of the maximal value. An increase of aberrations is probable in the case of simultaneous beam deflection and focusing, but the compact octupole system still offers the possibilities of astigmatism and field curvature correction. For the time being, the authors have only an intuitive image of the complex field distribution and its influence on the trajectories of charged particles in so compact an optical unit, but they will presently start a vast program of numerical investigations to gain further knowledge. Thus, the paper is mainly devoted to the deflecting function of the unit, though the hard problem of the simultaneous focusing fidelity will be presented separately after the necessary data are collected.

An important aim of the experiments was to establish whether the test method and the test stand are appropriable for the desired purposes. A JSM-840 microscope with a digital imaging channel proved to be a good electron optical bench for the octupole deflector unit.

The developed electronic control system together with the software met requirements regarding the output parameters and reliability. But it would be a grand challenge to develop a complete program for beam deflection with precise correction of astigmatism and field curvature in the octupole deflecting and focusing system.

Acknowledgments

The work was partially financed by a statutory fund of the Wrocław University of Technology and by the National Science Centre Poland, project no. UMO-2016/21/B/ST7/02216.

ORCID iDs

Marcin Białas https://orcid.org/0000-0003-2152-6303

References

[1] Orloff J, Swanson L and Utlaut M 2012 *High Resolution Focused Ion Beams: FIB and its Applications* (Berlin: Springer) p 304
[2] Giannuzzi L A and Stevens F A 2004 *Introduction to Focused Ion Beams: Instrumentation, Theory, Techniques and Practice* (Berlin: Springer)
[3] Slówko W and Wiatrowski A 2016 Coaxial ion microsource for VP/ESEM—E-beam impact mode *Vacuum* **132** 53–61
[4] Krysztof M, Grzebyk T P, Górecka-Drzazga A, Adamski K and Dziuban J 2018 Electron optics column for a new MEMS-type transmission electron microscope *Bull. Polish Acad. Sci. Tech. Sci.* **66** 133–7
[5] Tsuno K and Ioanoviciu D 2013 *The Wien Filter. Advances in Imaging and Electron Physics* vol 176 (New York: Elsevier) pp 177–212
[6] Tsuno K 1994 Simulation of a Wien filter as beam separator in a low-energy electron microscope *Ultramicroscopy* **55** 127–40
[7] Mook H W and Kruit P 1999 Optics and design of the fringe field monochromator for a Schottky field emission gun *Nucl. Instrum. Methods Phys. Res.* A **427** 109–20
[8] Szymanski H, Friedel K and Slówko W 1972 *Mikroobróbka wiązką elektronową (Electron Beam Micro-Machining)* (Warsaw: WNT)
[9] Kanaya K and Baba N 1980 A method of correcting the distorsed spot shape of a deflected electron probe by means of dynamic focusing and stigmator *J. Phys. E: Sci. Instrum.* **13** 415–26
[10] Baba N and Kanaya K 1981 Correction of the distorted electron beam spot deflected by electrostatic crossed deflection fields *J. Phys. E: Sci. Instrum.* **14** 183–93
[11] Otis Ch, Maazouz M, Logan D and Orloff J 2012 Pitfalls in the measurement of FIB beam size *Imaging Microsc.* www.imaging-git.com/science/electron-and-ion-microscopy/pitfalls-measurement-fib-beam-size (Accessed: 22 October 2012)
[12] Shorubalko I, Choi K, Stiefel M and Park H G 2017 Ion beam profiling from the interaction with a freestanding 2D layer *J. Nanotechnol.* **8** 682–7
[13] Harriott L R 1990 Beam-size measurements in focused ion beam systems *J. Vac. Sci. Technol.* A **8** 899
[14] Grigorov G N 1990 An 8-pole electrostatic deflection-system power supply *Meas. Sci. Technol.* **1** 651–3